Photon drag in a single-level metallic quantum well

Ole Keller

Institute of Physics, University of Aalborg, DK-9220 Aalborg Øst, Denmark

(Received 21 December 1992; revised manuscript received 29 March 1993)

A theoretical study of the photon-drag effect in a one-level metallic quantum well is presented. It is demonstrated that the photon drag, associated with second-order nonlinearities in the two-dimensional electron-gas system, originates in a combined diamagnetic and paramagnetic response. The photon-drag current density along the quantum well and the prevailing dc electric field across the well are calculated in a manner which takes into account local-field effects in the induced dc field as well as in the fundamental field of light. The local-field phenomena at the excitation frequency are studied on the basis of a self-consistent integral equation formalism. Within the framework of the slave and self-field approximations the photon-drag current density and the dc field prevailing across the well are examined. Finally, numerical results for the integrated photon-drag current density in a 3-Å-wide niobium quantum well deposited on a crystalline quartz substrate are presented. Data are obtained in the ~ 10-μm wavelength regime for both bulk and surface-wave excitation schemes.

I. INTRODUCTION

In recent years, the linear optical properties of so-called ultrathin metallic films deposited on dielectric substrates have been investigated experimentally[1,2] and theoretically.[3,4] The attractiveness of these systems is associated with the fact that the (few) monolayer thick films form metallic quantum wells. The confinement of the conduction-electron motion perpendicular to the plane of the film can give rise to a strong frequency dispersion of the reflectivity,[1] and hence to large changes in the *s*- and *p*-polarized reflection coefficients in certain wavelength ranges. Furthermore, the linear optical properties can change drastically with the thickness of the quantum well.[1] From a theoretical point of view, the metallic quantum wells are of considerable interest because they allow studies of a number of fundamental subjects in optics, e.g., local-field effects, two-dimensional jellium electrodynamics, mesoscopic phenomena, and few-level dynamics. As far as the few-level electrodynamics is concerned, it is possible in a narrow metallic quantum well to have only one bound state. If such a system is excited by light having a frequency far below that needed for photoemission, only the diamagnetic effect plays a role for the optical response of the quantum well, and even in the case of quantum wells with more than one bound state the diamagnetic response will dominate the electrodynamics if the frequency of the light is so low that no transitions can take place between the discrete levels. In fact, it has turned out that extremely good agreement between theory and experiment can be obtained in the (far) infrared regime where the diamagnetic effect is the dominating one.[1,3,4] In the case of two bound states in the metallic quantum well, basic local-field phenomena associated with the paramagnetic effect can be investigated.

Keeping in mind that the optical second-harmonic generation from centrosymmetric media is surface sensitive on the monolayer level (for a review, see Ref. 5), it appears natural and important to extend the studies of metal overlayers on dielectric substates to the nonlinear regime. Thus, a preliminary theoretical study of the second-harmonic generation from niobium quantum wells has recently been put forward by Liu and Keller.[6] One would expect that quantum-well effects in certain cases can play a role for metallic overlayers deposited on semiconductor or metal substrates. Second-harmonic generation investigations of these systems have also been on the rise for some years.[7–11]

In the present work, a theoretical study of the photon-drag effect, inevitably accompanying second-harmonic generation (and higher even-order nonlinearities), has been carried out for quantum wells of the metal-dielectric type within the framework of a nonlocal scattering-theory formalism for mesoscopic systems.[12] The photon-drag effect in two-dimensional electron-gas systems also has been studied recently theoretically by Vas'ko,[13] Luryi,[14] and Grinberg and Luryi,[15] and experimentally by Wieck, Sigg, and Ploog.[16] In semiconductor heterostructures, Stockman, Pandey, and George[17] have carried out a theoretical analysis. In previous studies of the photon-drag effect in confined structures the main emphasis was devoted to the effects that occur when the optical excitation frequency is close to an intersubband transition. Here, we focus our considerations on the simplest quantum wells, viz., the ones where only one bound (and occupied) state exists in the well, and we pay special attention to the role of local-field effects, which are known to play a prominent role for the linear electrodynamics of quantum wells in the diamagnetic regime. The two-band light-induced free-electron drift in metals was very recently investigated theoretically by Shalaev, Douketis, and Moskovits,[18] who also presented experimental evidence for the effect in the form of spatially asymmetric photoemission from silver films. An experimental study of the picosecond response of photon-drag detectors in the 10-μm wavelength range of the $Al_xGa_{1-x}As/GaAs$ multiple-quantum-well type has been presented by Kesselring *et al.*[19]

The paper is organized as follows. Taking as a starting point the Liouville equation for the many-body density-matrix operator, we establish, within the framework of the relaxation-time approximation, a general expression for the forced part of the second-order dc current density in Sec. II. When specializing in the case where the quantum well contains one bound state only, it is realized that only so-called semilocal processes, i.e., processes consisting of a combination of the diamagnetic and paramagnetic responses, contribute to the nonlinear dynamics of the two-dimensional electron gas. The semilocal photon-drag response tensor is calculated and analyzed in the low-temperature limit. The section is terminated by a calculation of the photon-drag current density across the quantum well. In Sec. III, the prevailing dc electric field inside the quantum well is calculated in a self-consistent manner. Due to the fact that the photon-drag current density and the local electric dc field depend crucially on the p-polarized first-harmonic local field in the well, we take up a study of the local field associated with the fundamental frequency in Sec. IV. A nonlocal calculation of the linear conductivity tensor of a single-level quantum well is performed, and the basic integral equations for the s- and p-polarized parts of the local field are studied. Special emphasis is devoted to an analysis of the p-polarized local field in the slave model. In this model the component of the local field perpendicular to the quantum well is driven (slaved) by the background field plus the field generated by the current density along the well in an approximation where this current density is independent of the local field across the well.[3] The slave approximation is analytically simple to handle and leads, in general, to accurate quantitative results.[3,4] In Sec. V, we use the slave model to calculate the photon-drag current density and the local dc field prevailing across the quantum well. Also, a few remarks concerning the self-field approximation are given. Finally, we discuss within the framework of the slave model the local-field resonances expected to appear in the photon drag associated with a single-level quantum well. In Sec. VI, numerical results are presented for a niobium quantum well of thickness 3 Å deposited on a crystalline quartz substrate. Using a bulk-wave excitation scheme the normalized integrated photon-drag current density is calculated as a function of frequency in the vicinity of the CO_2 laser lines for different angles of incidence. If electromagnetic surface waves are used to excite the photon-drag current it is demonstrated that the normalized drag current can be increased by two orders of magnitude near resonance. Special attention is paid to a comparison of the results of the slave and self-field models. In all the numerical studies the incident field is p polarized.

II. PHOTON-DRAG RESPONSE

A. Second-order dc current density: General expression

In order to calculate the nonlinear dc current density $\mathbf{J}_0(\mathbf{r})$ induced, at the position $\mathbf{r}$ in the quantum well, by a monochromatic (cyclic frequency ω) local field described by the vector potential,

$$\mathbf{A}_1(\mathbf{r},t)=\tfrac{1}{2}[\,\mathbf{A}_1(\mathbf{r};\omega)e^{-i\omega t}+\text{c.c.}\,] , \tag{1}$$

one takes as a starting point the general expression[20]

$$\mathbf{J}_0=\text{Tr}\{\rho_0\mathcal{J}_F\}+\tfrac{1}{4}\text{Tr}\{\rho_1\mathcal{J}_1^\dagger\}+\tfrac{1}{4}\text{Tr}\{\rho_1^\dagger\mathcal{J}_1\} . \tag{2}$$

This expression, valid to second order in the vector potential, is derived from an iterative solution of the Liouville equation for the many-body density-matrix operator. The quantities ρ_1 and ρ_0 denote the linear amplitude and the nonlinear dc part of the density-matrix operator, respectively, and $\mathcal{J}_F$ and $\mathcal{J}_1$ are the free (F) and field-perturbed parts of the current-density operator (in second quantization). The dagger stands for Hermitian conjugation, and Tr{ } means trace of { }. Denoting the field-unperturbed many-body states of the quantum well by $|I\rangle$, $|J\rangle$, etc., the associated energies by $E_IE_J,\ldots,$ and the probabilities for the various states being occupied by $P_I,P_J,\ldots,$ one has in the relaxation-time approximation,

$$\text{Tr}\{\rho_1\mathcal{J}_1^\dagger\}=[\text{Tr}\{\rho_1^\dagger\mathcal{J}_1\}]^*=\sum_{I,J}\frac{P_J-P_I}{\hbar(\omega+i/\tau)+E_J-E_I}\langle I|\mathcal{H}_1|J\rangle\langle J|\mathcal{J}_1^\dagger|I\rangle , \tag{3}$$

and

$$\begin{aligned}\text{Tr}\{\rho_0\mathcal{J}_F\}=&\sum_{I,J}\frac{P_J-P_I}{E_J-E_I+i\hbar/\tau}\langle I|\mathcal{H}_0|J\rangle\langle J|\mathcal{J}_F|I\rangle\\&+\tfrac{1}{4}\sum_{I,J,M}\frac{1}{E_J-E_I-i\hbar/\tau}\Bigg[\left[\frac{P_I-P_M}{E_M-E_I+\hbar(\omega+i/\tau)}+\frac{P_J-P_M}{E_J-E_M-\hbar(\omega+i/\tau)}\right]\langle I|\mathcal{H}_1|M\rangle\langle M|\mathcal{H}_1^\dagger|J\rangle\\&+\left[\frac{P_I-P_M}{E_M-E_I-\hbar(\omega+i/\tau)}+\frac{P_J-P_M}{E_J-E_M+\hbar(\omega+i/\tau)}\right]\\&\times\langle I|\mathcal{H}_1^\dagger|M\rangle\langle M|\mathcal{H}_1|J\rangle\Bigg]\langle J|\mathcal{J}_F|I\rangle ,\end{aligned} \tag{4}$$

where H_1 and H_0 denote the linear and the nonlinear dc part of the Hamiltonian, respectively.

B. Second-order dc current density: Single-level quantum well

Let us now consider a metallic quantum well in the form of a thin plane-parallel film of thickness $\sim d$ placed on top of a semi-infinite nonconducting substrate occupying the halfspace $z>0$ in a Cartesian xyz-coordinate system (see Fig. 1), and let us assume that there exists only one quantum level of energy ϵ in the quantum well and that this level lies below the Fermi level, i.e., $\epsilon<\epsilon_F$, ϵ_F denoting the Fermi energy of the particles (electrons). Parallel to the plane of the film it is assumed that the electrons exhibit free-electron-like behavior with an effective mass m. Limiting ourselves to a one-electron description, the particles in the quantum well have stationary-state wave functions of the form

$$\Psi(\mathbf{r})=(2\pi)^{-1}\psi(z)e^{i\mathbf{k}_\parallel\cdot\mathbf{r}} , \tag{5}$$

where $\psi(z)$ denotes the one-dimensional wave function of the only bound state, and $(2\pi)^{-1}\exp(i\mathbf{k}_\parallel\cdot\mathbf{r})$ describes the free-electron behavior of a particle having a wave vector $\mathbf{k}_\parallel$ along the film plane. It is possible to choose $\psi(z)$ to be real and we shall do so in the remaining part of this paper.

In the following it is assumed that the frequency of the prevailing electromagnetic field is so low that the electrons in the quantum well cannot be excited into the continuum. In this case, where one essentially has a two-dimensional free-electron gas, it can be shown, using arguments of the type given for the superconducting three-dimensional jellium case in Ref. 20, that the contribution from the term $\mathrm{Tr}\{\rho_0\mathcal{J}_F\}$ vanishes. Thus, for the single-level metallic quantum well the current density associated with the photon-drag effect is to be obtained from

$$\mathbf{J}_0(\mathbf{r})=\tfrac{1}{4}\mathrm{Tr}\{\rho_1\mathcal{J}_1^\dagger\}+\text{c.c.} \tag{6}$$

By taking advantage of the fact that our system exhibits infinitesimal translational invariance against displacements parallel to the xy plane, the vector potential amplitude of the local field stemming from a plane incident wave takes the form

$$\mathbf{A}_1(\mathbf{r};\omega)=\mathbf{A}_1(z;\mathbf{q}_\parallel,\omega)e^{i\mathbf{q}_\parallel\cdot\mathbf{r}} , \tag{7}$$

where $\mathbf{q}_\parallel$ is the component parallel to the surface of the wave vector of the incident field. In the gauge used to derive the expressions in Eqs. (3) and (4), the time-dependent part of the scalar potential was set equal to zero. Hence, the z part of the fundamental electric-field amplitude $\mathbf{E}_1(\mathbf{r};\omega)=\mathbf{E}_1(z;\mathbf{q}_\parallel,\omega)\exp(i\mathbf{q}_\parallel\cdot\mathbf{r})$ will be given by

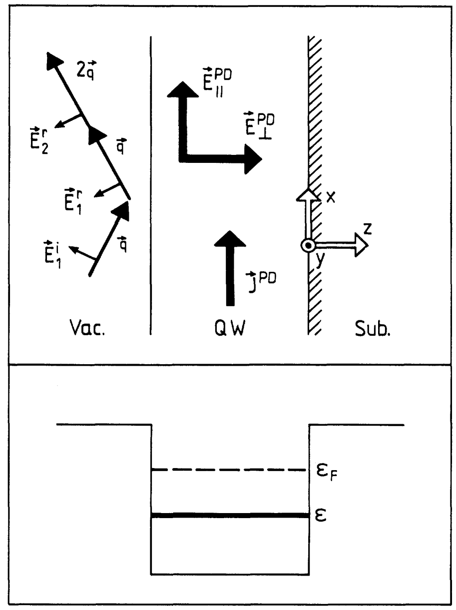

FIG. 1. Schematic figure showing a metallic quantum well (QW), in the form of a thin plane-parallel film, placed on top of a dielectric substrate (sub.). A p-polarized field ($\mathbf{E}_1^i$) of wave-vector $\mathbf{q}$ incident from the vacuum (vac.) side gives rise to first-harmonic ($\mathbf{E}_1^r$) and second-harmonic ($\mathbf{E}_2^r$) components in the reflected field. The nonlinear process is accompanied by the generation of a photon-drag (PD) current density ($\mathbf{J}^{\mathrm{PD}}$) along the quantum well, and a dc electric field ($\mathbf{E}_\parallel^{\mathrm{PD}}+\mathbf{E}_\perp^{\mathrm{PD}}$) in the plane of incidence. As indicated in the bottom part of the figure it is assumed that there exists only one bound energy eigenstate in the quantum well, and that this state lies below the Fermi energy, i.e., $\epsilon<\epsilon_F$.

$$\mathbf{E}_1(z;\mathbf{q}_\parallel,\omega)=i\omega\,\mathbf{A}_1(z;\mathbf{q}_\parallel,\omega) . \tag{8}$$

In the following, we shall for brevity normally neglect the superfluous indices $\mathbf{q}_\parallel$ and ω from our notation, i.e., $\mathbf{E}_1(z;\mathbf{q}_\parallel,\omega)=\mathbf{E}_1(z)$, etc. The translational invariance implies that the photon-drag current density in Eq. (6) becomes independent of x and y, i.e., $\mathbf{J}_0(\mathbf{r})=\mathbf{J}_0(z)$.

Using the single-particle wave function in Eq. (5) together with the expression for the vector potential in Eq. (7) [and the formula for $\mathcal{H}_1$ and $\mathcal{J}_1^\dagger$ (Ref. 12)], one can by standard calculations obtain the following explicit expression for the z-dependent photon-drag current density:

$$\mathbf{J}_0(z)=\tfrac{1}{2}\int\int_{\mathrm{QW}}\overleftrightarrow{\Sigma}_0(z,z',z''):\mathbf{E}_1(z'')\mathbf{E}_1^*(z')dz''dz'+\text{c.c.} , \tag{9}$$

where the so-called second-order photon-drag response tensor is given by

$$\overleftrightarrow{\Sigma}_0(z,z',z'')\equiv\overleftrightarrow{\Sigma}_0(z,z',z'';\mathbf{q}_\parallel,\omega)=-\frac{\hbar e^3\overleftrightarrow{\mathrm{U}}}{4m^2\omega^2}\psi^2(z)\psi^2(z'')\delta(z-z')$$
$$\times\int_{-\infty}^{\infty}\frac{f_0\left[\epsilon+\dfrac{\hbar^2}{2m}|\mathbf{k}_\parallel-\mathbf{q}_\parallel|^2\right]-f_0\left[\epsilon+\dfrac{\hbar^2k_\parallel^2}{2m}\right]}{\hbar(\omega+i/\tau)+\dfrac{\hbar^2}{2m}|\mathbf{k}_\parallel-\mathbf{q}_\parallel|^2-\dfrac{\hbar^2k_\parallel^2}{2m}}(2\mathbf{k}_\parallel-\mathbf{q}_\parallel)\frac{d^2k_\parallel}{(2\pi)^2} . \tag{10}$$

In Eq. (9) the integrations extend over the quantum well (QW), and in Eq. (10), $f_0(E)=\{\exp[(E-\mu)/k_B T]+1\}^{-1}$ is the Fermi-Dirac distribution function, $\overleftrightarrow{U}$ is the unit tensor of dimension 3×3, and $\delta(z-z')$ is the Dirac δ function. It is interesting to note that $\overleftrightarrow{\Sigma}_0$, apart from a factor of -1 is identical to the so-called semilocal (sl) diamagnetic nonlinear response tensor $\overleftrightarrow{\Sigma}_2^{(\mathrm{sl})}$ describing a part of the second-harmonic response from a two-dimensional electron gas, i.e.,[12]

$$\overleftrightarrow{\Sigma}_2^{(\mathrm{sl})}(z,z',z'';\mathbf{q}_\parallel,\omega)=-\overleftrightarrow{\Sigma}_0(z,z',z'';\mathbf{q}_\parallel,\omega) . \tag{11}$$

C. Photon-drag response tensor and current density

For the normal metallic state it is a good approximation to assume that the distribution function is a step function, i.e., $f_0(E)=1$ for $E<\epsilon_F$ and $f_0(E)=0$ for $E>\epsilon_F$. Using this $T=0$ approximation it is possible to carry out the double integral in Eq. (10) (see the Appendix). Doing this, one obtains

$$\overleftrightarrow{\Sigma}_0(z,z',z'')=\frac{\hbar e^3}{4m^2\omega^2}\times\psi^2(z)\psi^2(z'')\delta(z-z')(R_+-R_-)\overleftrightarrow{U}\mathbf{e}_x , \tag{12}$$

where

$$R_\pm=\frac{1}{2\pi\beta}\left\{\frac{1}{\beta}\left[\frac{2\alpha_\pm}{\beta}\mp q_\parallel\right][\alpha_\pm-\sqrt{\alpha_\pm^2-\beta^2\kappa_\parallel^2}]-\kappa_\parallel^2\right\} \tag{13}$$

with

$$\alpha_\pm=\hbar\left[\omega+\frac{i}{\tau}\right]\pm\frac{\hbar^2}{2m}q_\parallel^2 , \tag{14}$$

$$\beta=\frac{\hbar^2}{m}q_\parallel , \tag{15}$$

and

$$\kappa_\parallel=\left[\frac{2m}{\hbar^2}(\epsilon_F-\epsilon)\right]^{1/2} . \tag{16}$$

In Eq. (12), $\mathbf{e}_x$ denotes a unit vector in the positive x direction. In passing one should note that the last term in the curly brackets of Eq. (13), i.e., $\kappa_\parallel^2$, does not contribute to R_+-R_-.

It appears from Eq. (12), and it holds even if the low-temperature approximation is not made, that the third-rank photon-drag response tensor only has three nonvanishing tensor elements ($\sim\mathbf{e}_x\mathbf{e}_x\mathbf{e}_x$, $\mathbf{e}_y\mathbf{e}_y\mathbf{e}_x$, and $\mathbf{e}_z\mathbf{e}_z\mathbf{e}_x$) which furthermore are identical, cf. Fig. 2. It also transpires from this equation (and it is also correct for a nonsharp distribution function) that the photon-drag response tensor is semilocal, which means that the current density at z depends on the electric field in neighboring points only as far as one of the two $\mathbf{E}$ fields entering Eq. (9) is concerned. The spatial structure of the semilocal response function is shown schematically in Fig. 2.

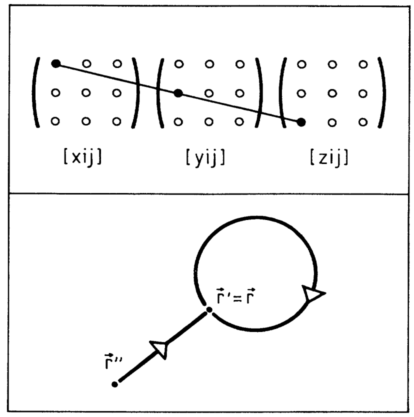

FIG. 2. Schematic diagram showing in the upper part the symmetry scheme of the third-rank photon-drag response tensor, and in the lower part the semilocal structure of the response. In a semilocal process the induced dc current density at space point $\mathbf{r}$ depends on the product of the fundamental electric field in the surroundings (straight line, $\mathbf{r}''\to\mathbf{r}$) and at $\mathbf{r}$ (circle, $\mathbf{r}'=\mathbf{r}$).

By inserting Eq. (12) into (9) the photon-drag current density takes the form

$$\mathbf{J}_0(z)=\frac{1}{2}\left\{K(q_\parallel,\omega)\psi^2(z)\mathbf{E}_1^*(z)\times\int_{\mathrm{QW}}\psi^2(z')E_{1,x}(z')dz'+\mathrm{c.c.}\right\} \tag{17}$$

with

$$K(q_\parallel,\omega)=\frac{\hbar e^3}{4m^2\omega^2}(R_+-R_-) . \tag{18}$$

It is readily demonstrated that $R_+-R_-\to 0$ for $q_\parallel\to 0$ so that

$$K(q_\parallel\to 0,\omega)=0 . \tag{19}$$

This means that the photon-drag current density vanishes in the long-wavelength (local) limit, an expected result since there cannot be any net moment exchange between the electrons and the light in this limit. The photon-drag effect also is absent if the prevailing fundamental electromagnetic field is s polarized. As is well known the prevailing fundamental field is s polarized if the incident electric field is s polarized; cf. also the discussion in Sec. IV.

III. PREVAILING dc ELECTRIC FIELD ACROSS THE QUANTUM WELL

In Sec. II, an expression [Eq. (17)] was derived for the *forced* part of the photon-drag current density. To this part one has to add an as yet unknown *free* (F) part $\mathbf{J}_F$ in order to obtain a self-consistent solution to the combined set of the Schrödinger and Maxwell equations including the appropriate boundary conditions. The translational invariance parallel to the xy plane implies that the prevailing dc magnetic field and the free current density are functions of z only, i.e., $\mathbf{B}_0=\mathbf{B}_0(z)$ and $\mathbf{J}_F=\mathbf{J}_F(z)$, respectively. In turn, it follows from the Maxwell equation

$$\nabla\times\mathbf{B}_0(z)=\mu_0[\mathbf{J}_F(z)+\mathbf{J}_0(z)] \quad (20)$$

that the total current density in the direction perpendicular to the quantum well vanishes, i.e.,

$$\mathbf{e}_z\cdot[\mathbf{J}_F(z)+\mathbf{J}_0(z)]=0 , \quad (21)$$

$\mathbf{e}_z$ being a unit vector in the z direction. If the electrons are allowed to flow freely (i.e., without externally impressed dc fields) along the quantum well the associated current density is given by $(\overleftrightarrow{\mathbf{U}}-\mathbf{e}_z\mathbf{e}_z)\cdot\mathbf{J}_0(z)$.

Since the total dc current density in the z direction vanishes, a dc electric field, $\mathbf{E}_0(z)=E_{0,z}(z)\mathbf{e}_z$, must necessarily be created across the quantum well. To determine this field we shall make use of the fact that the free current density in the z direction is related to $E_{0,z}(z)$ via a constitutive equation of the form

$$J_{F,z}(z)=\int_{\mathrm{QW}}\sigma_{zz}(z,z';\omega=0)E_{0,z}(z')dz' , \quad (22)$$

where $\sigma_{zz}(z,z';\omega=0)$ is the relevant linear dc conductivity response function. For our one-level quantum well, σ_{zz} is

$$\sigma_{zz}(z,z';\omega=0)=\frac{\tau e^2}{m}n(z)\delta(z-z') , \quad (23)$$

where

$$n(z)=\frac{m}{\pi\hbar^2}(\epsilon_F-\epsilon)\psi^2(z) , \quad \epsilon<\epsilon_F \quad (24)$$

is the electron density. The results in Eqs. (22)–(24) are derived in Sec. IV. By combining Eqs. (17) and (21)–(24) it is realized that the dc field induced across the quantum well is given by

$$E_{0,z}(z)=\frac{\pi\hbar^2}{2e^2\tau(\epsilon-\epsilon_F)}\left\{K(q_\parallel,\omega)E^*_{1,z}(z)\times\int_{\mathrm{QW}}\psi^2(z')E_{1,x}(z')dz'+\text{c.c.}\right\} . \quad (25)$$

IV. LOCAL FIELD AT THE FUNDAMENTAL FREQUENCY

A. Linear conductivity response tensor

In order to achieve an explicit determination of the dc field generated across the quantum well and the current density induced along the well one has to calculate the local field at the fundamental frequency. As a starting point let us consider the linear conductivity response tensor for a single-level quantum well, i.e.,[12]

$$\overleftrightarrow{\sigma}(z,z';\mathbf{q}_\parallel,\omega)=\frac{e^2\tau}{m(1-i\omega\tau)}n(z)\delta(z-z')\overleftrightarrow{\mathbf{U}}+\frac{ie^2\hbar^2}{2m^2\omega}\psi^2(z)\psi(z')\int_{-\infty}^{\infty}\frac{f_0\left[\epsilon+\frac{\hbar^2}{2m}|\mathbf{k}_\parallel-\mathbf{q}_\parallel|^2\right]-f_0\left[\epsilon+\frac{\hbar^2k_\parallel^2}{2m}\right]}{\hbar(\omega+i/\tau)+\frac{\hbar^2}{2m}|\mathbf{k}_\parallel-\mathbf{q}_\parallel|^2-\frac{\hbar^2k_\parallel^2}{2m}}(2\mathbf{k}_\parallel-\mathbf{q}_\parallel)(2\mathbf{k}_\parallel-\mathbf{q}_\parallel)\frac{d^2k_\parallel}{(2\pi)^2} , \quad (26)$$

where the electron density is given by

$$n(z)=2\psi^2(z)\int_{-\infty}^{\infty}f_0\left[\epsilon+\frac{\hbar^2}{2m}k_\parallel^2\right]\frac{d^2k_\parallel}{(2\pi)^2}=\frac{mk_BT}{\pi\hbar^2}\psi^2(z)\ln\left[1+\exp\left[\frac{\epsilon_F-\epsilon}{k_BT}\right]\right], \quad \epsilon<\epsilon_F . \quad (27)$$

In the low-temperature limit, the expression for the density reduces to that cited in Eq. (24). It is possible in the $T\rightarrow 0$ limit to perform the integrations in Eq. (26), cf. the Appendix. The result one obtains is the following:

$$\overleftrightarrow{\sigma}=\begin{bmatrix}\sigma_{xx} & 0 & 0\\ 0 & \sigma_{yy} & 0\\ 0 & 0 & \sigma_{zz}\end{bmatrix} , \quad (28)$$

where

$$\sigma_{xx}(z,z';q_\parallel,\omega)=\frac{e^2\tau}{m(1-i\omega\tau)}n(z)\delta(z-z')+\frac{2ie^2\hbar^2}{m^2\omega}\psi^2(z)\psi^2(z')(S_--S_+) , \quad (29)$$

$$\sigma_{yy}(z,z';q_\parallel,\omega)=\frac{e^2\tau}{m(1-i\omega\tau)}n(z)\delta(z-z')+\frac{2ie^2\hbar^2}{m^2\omega}\psi^2(z)\psi^2(z')(T_--T_+) , \quad (30)$$

and

$$\sigma_{zz}(z,z';q_\parallel,\omega)=\frac{e^2\tau}{m(1-i\omega\tau)}n(z)\delta(z-z') \quad (31)$$

with $n(z)$ being given by Eq. (24). The wave-vector dependence of $\overleftrightarrow{\sigma}$ is contained in the quantities

$$S_\pm(q_\parallel,\omega)=\frac{1}{2\pi\beta^2}\left[\frac{\alpha_\pm}{\beta}\mp\frac{q_\parallel}{2}\right]^2[\alpha_\pm-\sqrt{\alpha_\pm^2-\beta^2\kappa_\parallel^2}]-\frac{\kappa_\parallel^2}{4\pi\beta}\left[\frac{\alpha_\pm}{\beta}\mp q_\parallel\right] \tag{32}$$

and

$$T_\pm(q_\parallel,\omega)=\frac{\alpha_\pm}{2\pi\beta^2}\left\{\frac{1}{3\beta^2\alpha_\pm}[(\alpha_\pm^2-\beta^2\kappa_\parallel^2)^{3/2}-\alpha_\pm^3]+\frac{\kappa_\parallel^2}{2}\right\}. \tag{33}$$

One notices that the conductivity tensor is diagonal. In general, i.e., in cases where several levels are present and interband transitons are thus allowed, the elements σ_{xz} and σ_{zx} are different from zero. The elements σ_{xy}, σ_{yx}, σ_{yz}, and σ_{zy} always vanish since the *s*- and *p*-polarized excitations are uncoupled. The reason that σ_{xz} and σ_{zx} are zero here stems from the fact that when only one level is present the electron motion in the *z* direction is frozen implying in turn that the *z* component of the transition current density vanishes. Since the *z* component of the transition current is zero, σ_{zz} consists only of the local (i.e., $q_\parallel$ independent) diamagnetic contribution. In the static limit, σ_{zz} of Eq. (31) is reduced to the expression given in Eq. (23). The nonlocal (paramagnetic) terms entering the expressions for σ_{xx} and σ_{yy} are different ($S_\pm\neq T_\pm$) because the electron motions along the *x* and *y* directions are no longer equivalent when $q_\parallel\neq 0$. It readily appears from Eq. (26) that the paramagnetic contributions to σ_{xx} and σ_{yy} vanish in the limit $q_\parallel\to 0$. Hence, in the local limit only the diamagnetic term survives and $\sigma_{xx}=\sigma_{yy}=\sigma_{zz}$, as expected.

B. Solution of the basic integral equations for the local field

With a knowledge of the linear conductivity response tensor, the local electric field at the fundamental frequency can be obtained by solving the basic integral equation[12]

$$\mathbf{E}_1(z)=\mathbf{E}_1^B(z)-i\mu_0\omega\int\int_{QW}\overleftrightarrow{G}^B(z,z')\cdot\boldsymbol{\sigma}(z',z'')\cdot\mathbf{E}_1(z'')dz''dz' , \tag{34}$$

where $\overleftrightarrow{G}^B$ is the relevant electromagnetic Green's function of the vacuum-substrate system, and $\mathbf{E}_1^B$ is the so-called background field (consisting of the sum of the incident field and the field reflected from the substrate). The tensorial forms of the Green's function and the conductivity [Eq. (28)] allow us to divide the integral equation in (34) into decoupled equations for the *s*- and *p*-polarized components of the fundamental field, i.e.,

$$E_{1,y}(z)=E_{1,y}^B(z)-i\mu_0\omega\int\int_{QW}G_{yy}^B(z,z')\sigma_{yy}(z',z'')\times E_{1,y}(z'')dz''dz' , \tag{35}$$

and

$$E_{1,x}(z)=E_{1,x}^B(z)-i\mu_0\omega\int\int_{QW}[G_{xx}^B(z,z')\sigma_{xx}(z',z'')E_{1,x}(z'')+G_{xz}^B(z,z')\sigma_{zz}(z',z'')E_{1,z}(z'')]dz''dz' , \tag{36}$$

$$E_{1,z}(z)=E_{1,z}^B(z)-i\mu_0\omega\int\int_{QW}[G_{zx}^B(z,z')\sigma_{xx}(z',z'')E_{1,x}(z'')+G_{zz}^B(z,z')\sigma_{zz}(z',z'')E_{1,z}(z'')]dz''dz' , \tag{37}$$

respectively. Since the integrals in Eqs. (35)–(37) extend over the quantum well the basic problem consists of finding a self-consistent solution for the local field *inside* the quantum well. Once this has been obtained the field outside the quantum well, if necessary, can be found by integration of *known* functions over the quantum well.

Let us start by considering the integral equation for the *s*-polarized part of the fundamental field. Since for the wavelengths of interest in the present context (optical ones) the electromagnetic propagator and the background field are almost constant across the quantum well, one has $E_{1,y}(z)\simeq E_{1,y}^B(0)\equiv E_{1,y}^B$ and

$$G_{yy}^B(z,z')\simeq G_{yy}^B(0,0)=(1+r^s)/(2iq_\perp^0) ,$$

where r^s is the amplitude reflection coefficient for *s*-polarized fields, and $q_\perp^0=[(\omega/c_0)^2-q_\parallel^2]^{1/2}$ is the component of the wave vector of the incident field perpendicular to the surface. In turn, this means that the local field is approximately constant across the well, i.e., $E_{1,y}(z)\simeq E_{1,y}(0)\equiv E_{1,y}$. Next, this implies that the solution of Eq. (35) is given by

$$E_{1,y}=E_{1,y}^B\left[1+i\mu_0\omega G_{yy}^B(0,0)\times\int\int_{QW}\sigma_{yy}(z',z'')dz''dz'\right]^{-1} \tag{38}$$

inside the quantum well. Utilizing the normalization of the wave function [$\int_{QW}|\psi(z)|^2dz=1$], it is a straightforward matter to carry out the double integral $\int\int_{QW}\sigma_{yy}(z',z'')dz''dz'$. Doing this, finally, one obtains

$$E_{1,y}=\frac{E_{1,y}^B}{1-K_{yy}} , \tag{39}$$

where

$$K_{yy}=e^2G_{yy}^B(0,0)\left[\frac{\mu_0\omega(\epsilon_F-\epsilon)}{\pi\hbar^2(\omega+i/\tau)}+\frac{2\mu_0\hbar^2(T_--T_+)}{m^2}\right]. \tag{40}$$

The result in Eq. (39) [with (40)] is for one level a generalization of that obtained recently in the local limit.[3] The local diamagnetic calculation performed in Ref. 3 was applied successfully to interpret recent linear infrared reflection data for a niobium quantum well deposited on a crystalline quartz substrate.[1]

Let us turn our attention now towards the coupled integral equations for the p-polarized part of the fundamental field. Thus, by inserting the expressions for σ_{xx} and σ_{zz} given in Eqs. (29) and (31), with $n(z)$ taken from Eq. (24), into Eqs. (36) and (37), and by extracting the self-field part, $(c_0/\omega)^2\delta(z-z')$, of the background propagator from G^B_{zz}, i.e.,

$$G^B_{zz}(z,z')=\left[\frac{c_0}{\omega}\right]^2\delta(z-z')+P^B_{zz}(z,z') , \tag{41}$$

the basic integral equations take the form

$$\begin{aligned}E_{1,x}(z)=E^B_{1,x}(z)-i\mu_0\omega\Bigg\{&\frac{e^2\tau(\epsilon_F-\epsilon)}{\pi\hbar^2(1-i\omega\tau)}\int_{\rm QW}G^B_{xx}(z,z')\psi^2(z')E_{1,x}(z')dz'\\&+\frac{2ie^2\hbar^2}{m^2\omega}(S_--S_+)\left[\int_{\rm QW}G^B_{xx}(z,z')\psi^2(z')dz'\right]\left[\int_{\rm QW}\psi^2(z'')E_{1,x}(z'')dz''\right]\\&+\frac{e^2\tau(\epsilon_F-\epsilon)}{\pi\hbar^2(1-i\omega\tau)}\int_{\rm QW}G^B_{xz}(z,z')\psi^2(z')E_{1,z}(z')dz'\Bigg\}\end{aligned} \tag{42}$$

and

$$\begin{aligned}E_{1,z}(z)=E^B_{1,z}(z)-i\mu_0\omega\Bigg\{&\frac{e^2\tau(\epsilon_F-\epsilon)}{\pi\hbar^2(1-i\omega\tau)}\int_{\rm QW}G^B_{zx}(z,z')\psi^2(z')E_{1,x}(z')dz'\\&+\frac{2ie^2\hbar^2}{m^2\omega}(S_--S_+)\left[\int_{\rm QW}G^B_{zx}(z,z')\psi^2(z')dz'\right]\left[\int_{\rm QW}\psi^2(z'')E_{1,x}(z'')dz''\right]\\&+\frac{c_0^2e^2\tau(\epsilon_F-\epsilon)}{\pi\hbar^2\omega^2(1-i\omega\tau)}\psi^2(z)E_{1,z}(z)+\frac{e^2\tau(\epsilon_F-\epsilon)}{\pi\hbar^2(1-i\omega\tau)}\int_{\rm QW}P^B_{zz}(z,z')\psi^2(z')E_{1,z}(z')dz'\Bigg\} .\end{aligned} \tag{43}$$

Since no double integrals occur in Eqs. (42) and (43), this coupled set of integral equations is considerably simpler to solve than the general set in Eqs. (36) and (37). A further reduction of the problem is obtained by utilizing that the background field and the propagator components G^B_{xx} and P^B_{zz} are slowly varying across the quantum well. Thus, in an explicit form,

$$G^B_{xx}(z,z')\simeq G^B_{xx}(0,0)=\frac{q^0_\perp}{2i}\left[\frac{c_0}{\omega}\right]^2(1-r^p) , \tag{44}$$

$$P^B_{zz}(z,z')\simeq P^B_{zz}(0,0)=\frac{q^2_\parallel}{2iq^0_\perp}\left[\frac{c_0}{\omega}\right]^2(1+r^p) , \tag{45}$$

$E^B_{1,x}(z)\simeq E^B_{1,x}(0)\equiv E^B_{1,x}$, and $E^B_{1,z}(z)\simeq E^B_{1,z}(0)\equiv E^B_{1,z}$, where r^p is the p-polarized amplitude reflection coefficient. The off-diagonal elements of the electromagnetic propagator are only slightly reduced in their spatial structure by the neglect of the slow variations. Thus,

$$G^B_{xz}(z,z')\simeq\frac{q_\parallel}{2i}\left[\frac{c_0}{\omega}\right]^2\mathcal{F}_+(z,z') \tag{46}$$

and

$$G^B_{zx}(z,z')\simeq\frac{q_\parallel}{2i}\left[\frac{c_0}{\omega}\right]^2\mathcal{F}_-(z,z') , \tag{47}$$

where

$$\mathcal{F}_\pm(z,z')=\Theta(z'-z)-\Theta(z-z')\pm r^p , \tag{48}$$

Θ being the Heaviside unit step function. By inserting the above-mentioned approximations into Eqs. (42) and (43), and by utilizing the normalization of $\psi(z)$, the fundamental set of coupled integral equations for the p-polarized case takes the form

$$E_{1,x}(z)=E^B_{1,x}+K_{xx}\int_{QW}\psi^2(z')E_{1,x}(z')dz'+A\int_{QW}\mathcal{F}_+(z,z')\psi^2(z')E_{1,z}(z')dz' , \tag{49}$$

$$E_{1,z}(z)=E^B_{1,z}+A\int_{QW}\mathcal{F}_-(z,z')\psi^2(z')E_{1,x}(z')dz'+U\left[\int_{QW}\mathcal{F}_-(z,z')\psi^2(z')dz'\right]\left[\int_{QW}\psi^2(z')E_{1,x}(z')dz'\right]$$
$$+V\psi^2(z)E_{1,z}(z)+W\int_{QW}\psi^2(z')E_{1,z}(z')dz' , \tag{50}$$

where

$$K_{xx}=\frac{e^2q^0_\perp(r^p-1)}{2\epsilon_0\omega}\left[\frac{\tau(\epsilon_F-\epsilon)}{\pi\hbar^2(1-i\omega\tau)}+\frac{2i\hbar^2(S_--S_+)}{m^2\omega}\right] , \tag{51}$$

$$A=\frac{q_\parallel e^2\tau(\epsilon-\epsilon_F)}{2\pi\epsilon_0\omega\hbar^2(1-i\omega\tau)} , \tag{52}$$

$$U=\frac{e^2\hbar^2q_\parallel(S_--S_+)}{i\epsilon_0 m^2\omega^2} , \tag{53}$$

$$V=\frac{e^2\tau(\epsilon_F-\epsilon)}{i\epsilon_0\omega\pi\hbar^2(1-i\omega\tau)} , \tag{54}$$

and

$$W=\frac{e^2\tau q^2_\parallel(\epsilon-\epsilon_F)(1+r^p)}{2\pi\epsilon_0 q^0_\perp\omega\hbar^2(1-i\omega\tau)} . \tag{55}$$

By numerical methods it is a straightforward task for reasonably simple choices of the one-electron wave function $\psi(z)$ to obtain the solution for the self-consistent field.

Instead of embarking on a general analysis which would bring us outside the scope of this paper, let us consider the solution of Eqs. (49) and (50) in a limiting case of conceptual interest. The freezing of the electron motion in the z direction implies that only the off-diagonal elements of the electromagnetic propagator are able to couple the x and z components of the local electric field. In the so-called slave approximation[3] which, at least in the $q_\parallel=0$ limit, has turned out to give results for the local field in extremely good agreement with those obtained by exact numerical calculations, the term containing $G^B_{xz}(\mathcal{F}_+)$ in Eq. (49) is neglected. Neglect of this term makes the integral equation for the local field along the quantum well independent of $E_{1,z}(z)$, i.e.,

$$E_{1,x}(z)=E^B_{1,x}+K_{xx}\int_{QW}\psi^2(z')E_{1,x}(z')dz' . \tag{56}$$

Since the right-hand side of this equation is independent of z, $E_{1,x}(z)$ must be independent of z and is given by

$$E_{1,x}=\frac{E^B_{1,x}}{1-K_{xx}} . \tag{57}$$

As one would expect, the solutions for $E_{1,x}$ (taking in the slave approximation [Eq. (57)]) and $E_{1,y}$ [Eq. (39)] have the same form. By inserting the solution in Eq. (57) into Eq. (50), the integral equation for $E_{1,z}(z)$ becomes

$$[1-V\psi^2(z)]E_{1,z}(z)=E^{B,\text{eff}}_{1,z}(z)+W\int_{QW}\psi^2(z')E_{1,z}(z')dz' , \tag{58}$$

where

$$E^{B,\text{eff}}_{1,z}(z)=E^B_{1,z}+\frac{(A+U)E_{1,x}}{1-K_{xx}}\int_{QW}\mathcal{F}_-(z,z')\psi^2(z')dz' \tag{59}$$

is an effective background field consisting of the impressed background field, $E^B_{1,z}$, and the field created by the self-consistent motion of the electrons along the quantum well (in an approximation where the effect of the field across the well is negligible). It readily appears that the solution for $E_{1,z}(z)$ in Eq. (58) must have the form

$$E_{1,z}(z)=\frac{E^{B,\text{eff}}_{1,z}(z)+WC}{1-V\psi^2(z)} , \tag{60}$$

where

$$C=\int_{QW}\psi^2(z')E_{1,z}(z')dz' \tag{61}$$

is a yet unknown constant. This constant can be obtained by inserting Eq. (60) into Eq. (61). Doing this, one obtains

$$C=\int_{QW}\frac{\psi^2(z)E^{B,\text{eff}}_{1,z}(z)dz}{1-V\psi^2(z)}\left[1-W\int_{QW}\frac{\psi^2(z)dz}{1-V\psi^2(z)}\right]^{-1} . \tag{62}$$

If one neglects all parts of the electromagnetic background propagator with the exception of the self-field part, $(c_0/\omega)^2\delta(z-z')\mathbf{e}_z\mathbf{e}_z$, the local field *inside* the quantum well is given by

$$E_{1,x}=E^B_{1,x} \quad \text{(SF approx.)} \tag{63}$$

and

$$E_{1,z}(z)=\frac{E^B_{1,z}}{1-V\psi^2(z)} \quad \text{(SF approx.)} . \tag{64}$$

While such an approximation certainly is too crude to be able to account for the linear p-polarized reflectivity which depends almost exclusively on the local field along the quantum well,[3,4] the self-field approximation describes the z component of the local field quite well at least in thin quantum wells.[4]

V. PHOTON DRAG IN THE SLAVE AND SELF-FIELD APPROXIMATIONS

A. Drag current and voltage

Within the framework of the slave approximation the photon-drag current density can be obtained by inserting Eqs. (39) and (57) into the expression $(\overleftrightarrow{\mathbf{U}}-\mathbf{e}_z\mathbf{e}_z)\cdot\mathbf{J}_0(z)$, taking $\mathbf{J}_0(z)$ from Eq. (17) and using the normalization of the wave function. Thus,

$$(\overleftrightarrow{\mathbf{U}}-\mathbf{e}_z\mathbf{e}_z)\cdot\mathbf{J}_0(z)=\frac{1}{2}\left\{K(q_\parallel,\omega)\psi^2(z)\frac{E^B_{1,x}}{1-K_{xx}}\times\left[\frac{E^B_{1,x}\mathbf{e}_x}{1-K_{xx}}+\frac{E^B_{1,y}\mathbf{e}_y}{1-K_{yy}}\right]^*+\text{c.c.}\right\} . \quad (65)$$

By integration of this result over the quantum well, one obtains the following expression for the integrated photon-drag current density $\mathbf{I}_0$:

$$\mathbf{I}_0=(\overleftrightarrow{\mathbf{U}}-\mathbf{e}_z\mathbf{e}_z)\int_{\text{QW}}\mathbf{J}_0(z)dz =\frac{1}{2}\left\{K(q_\parallel,\omega)\frac{E^B_{1,x}}{1-K_{xx}}\times\left[\frac{E^B_{1,x}\mathbf{e}_x}{1-K_{xx}}+\frac{E^B_{1,y}\mathbf{e}_y}{1-K_{yy}}\right]^*+\text{c.c.}\right\} . \quad (66)$$

By inserting Eqs. (39), (57), and (60) into Eq. (25) it is realized that the dc field induced perpendicular to the quantum well is given by

$$E_{0,z}(z)=\frac{\pi\hbar^2}{2e^2\tau(\epsilon-\epsilon_F)}\times\left\{K(q_\parallel,\omega)\frac{[E^{B,\text{eff}}_{1,z}(z)]^*+W^*C^*}{[1-V\psi^2(z)]^*}\times\frac{E^B_{1,x}}{1-K_{xx}}+\text{c.c.}\right\} \quad (67)$$

in the slave model. The dc voltage induced across the well becomes

$$V_0=-\frac{\pi\hbar^2}{2e^2\tau(\epsilon-\epsilon_F)}\times\left\{K(q_\parallel,\omega)\frac{E^B_{1,x}}{1-K_{xx}}\times\int_{\text{QW}}\frac{[E^{B,\text{eff}}_{1,z}(z)]^*+W^*C^*}{[1-V\psi^2(z)]^*}dz+\text{c.c.}\right\} . \quad (68)$$

A usually crude approximation for I_0 and V_0 can readily be obtained on the basis of the self-field approximation. Thus, by utilizing Eqs. (63) and (64) and by setting $E_{1,y}=0$, one obtains with $\mathbf{I}_0=I_0\mathbf{e}_x$ a photon-drag current

$$I_0=|E^B_{1,x}|^2\text{Re}\{K(q_\parallel,\omega)\} , \quad (69)$$

and a dc voltage

$$V_0=-\frac{\pi\hbar^2}{2e^2\tau(\epsilon-\epsilon_F)}\left\{K(q_\parallel,\omega)E^B_{1,x}(E^B_{1,z})^*\times\int_{\text{QW}}\frac{dz}{[1-V\psi^2(z)]^*}+\text{c.c.}\right\} . \quad (70)$$

B. Local-field resonances

It is known[12] that the eigenmodes of the full quantum-well system can be obtained from the basic integral equation in (34), setting $\mathbf{E}^B_1(z)=0$. This implies that the eigenmode condition for the s-polarized part of the field is, cf. Eq. (39),

$$K_{yy}=1 . \quad (71)$$

Within the framework of the slave model the p-polarized field exhibits two eigenmodes, one for the x component and one for the z component. The reason that the x and z resonances are decoupled originates in the slave approximation. The two p-polarized eigenmodes are readily obtained from the singularities of Eqs. (57) and (62), i.e., from the conditions

$$K_{xx}=1 \quad (72)$$

and

$$\int_{\text{QW}}\frac{\psi^2(z)dz}{1-V\psi^2(z)}=W^{-1} . \quad (73)$$

The eigenmode conditions $K_{xx}=1$ and $K_{yy}=1$ can cause resonances in the photon-drag current density (and the integrated current density), cf. Eq. (65) [and Eq. (66)]. The dc voltage induced across the well will be resonantly enhanced if $K_{xx}=1$ or if the condition in Eq. (73) is fulfilled. Also, the z component of the local field exhibits a resonance if one of these two requirements is met. In addition, it transpires from Eq. (67) that $E_{0,z}(z)$ should show a spatially localized resonance at $z=z_{\text{res}}$ provided the condition $V\psi^2(z_{\text{res}})=1$ can be fulfilled. In the collisionless ($\omega\tau\gg1$) limit this condition takes the explicit form

$$\psi^2(z_{\text{res}})=\frac{\pi\epsilon_0(\hbar\omega)^2}{e^2(\epsilon_F-\epsilon)} . \quad (74)$$

VI. NUMERICAL RESULTS

In the present section a numerical analysis of the photon-drag effect in a niobium quantum well deposited on a crystalline quartz substrate is carried out for photon energies in the range $1.0\lesssim\hbar\omega\lesssim1.8$ eV. The Nb-quartz quantum-well system has been chosen because recent local-field calculations [based on Eq. (35)] of the s- and p-polarized linear reflection coefficients[3,4] and of the electromagnetic surface-wave dispersion relation[4] have turned out to be in good agreement with the experimental data for these quantities for film thicknesses in the range $d \sim 3-25$ Å.[1] For all film thicknesses the best agreement is obtained by choosing an electron collision frequency $\tau^{-1}=3\times10^{14}$ s^{-1} ($\hbar/\tau=1.24$ eV). To compare with our one-level calculations a niobium film of thickness $d=3$ Å was used. For this film thickness there exists only one bound state below the Fermi level, and $\epsilon-\epsilon_F \simeq -3.31$ eV. In addition, one has an unoccupied ($T=300$ K) level (ϵ_2) above ϵ_F at $\epsilon_2-\epsilon_F \simeq 1.91$ eV, but in the photon-energy range of interest here the optical excitation of this level is completely negligible. The optical axis of the quartz substrate is placed perpendicular to the plane of incidence so that the p-polarized reflection coefficient is given by $r_p=(q_\perp^0\epsilon_Q-\kappa_\perp)/(q_\perp^0\epsilon_Q+\kappa_\perp)$, where $\kappa_\perp=[(\omega/c_0)^2\epsilon_Q-q_\parallel^2]^{1/2}$ is the wave-vector component of the (transmitted) field inside the quartz perpendicular to the surface. In the infrared region studied here, the pure quartz substrate exhibits a resonance in the reflection spectrum and in our calculations the associated frequency dependence of the complex dielectric constant ϵ_Q was used.[1,21] Below, the integrated photon-drag current density is calculated using (i) p-polarized bulk-wave and (ii) surface-wave excitation schemes.

A. Bulk-wave excitation of the drag current

For a p-polarized incident field the magnitude of the associated Poynting vector ($\mathbf{S}_{\text{inc}}$) at the vacuum-quartz interface is given by $S_{\text{inc}}=\frac{1}{2}\epsilon_0 c_0|E_{1,x}^0|^2/\cos^2\theta$, where θ is the angle of incidence and $E_{1,x}^0$ is the x component of the incident field. Utilizing that $E_{1,x}^B=E_{1,x}^0(1-r_p)$, it follows [cf. Eq. (66)] that the ratio between the magnitudes of the integrated photon-drag current density and the incident Poynting vector is given by

$$\frac{I_0}{S_{\text{inc}}}=\frac{2|1-r_p(q_\parallel,\omega)|^2\cos^2\theta}{\epsilon_0 c_0|1-K_{xx}(q_\parallel,\omega)|^2}\text{Re}K(q_\parallel,\omega) \tag{75}$$

within the framework of the slave approximation. In Fig. 3, the result of a numerical calculation of the ratio I_0/S_{inc} as a function of the photon energy for three different angles of incident ($\theta=20°$, 50°, and 70°) is shown. It appears from this figure that the drag current is largest in the frequency region where the p-polarized reflection spectrum of the quartz substrate has a resonance, cf. Ref. 3. If the x component of the local field at the fundamental field, $E_{1,x}$, is calculated on the basis of the "exact" equations [Eqs. (36) and (37)], it turns out[4] that the relative deviation [("exact"−slave)/slave] between the I_0/I_{inc} calculations for all ω and θ is less than 10^{-3}. The slave approximation is thus an extremely good approximation in the present case. As illustrated in Fig. 3, even the self-field approximation is quite accurate in the bulk-wave excitation scheme. The photon-drag current density varies appreciably with the angle of incidence as illustrated in Fig. 4 where the ratio I_0/S_{inc} has been plotted as a function of θ for three different frequencies ($\hbar\omega=0.12$, 0.15, and 0.17 eV). As in Fig. 3, the slave model has been used to calculate I_0/S_{inc} and a comparison is made to the self-field model also.

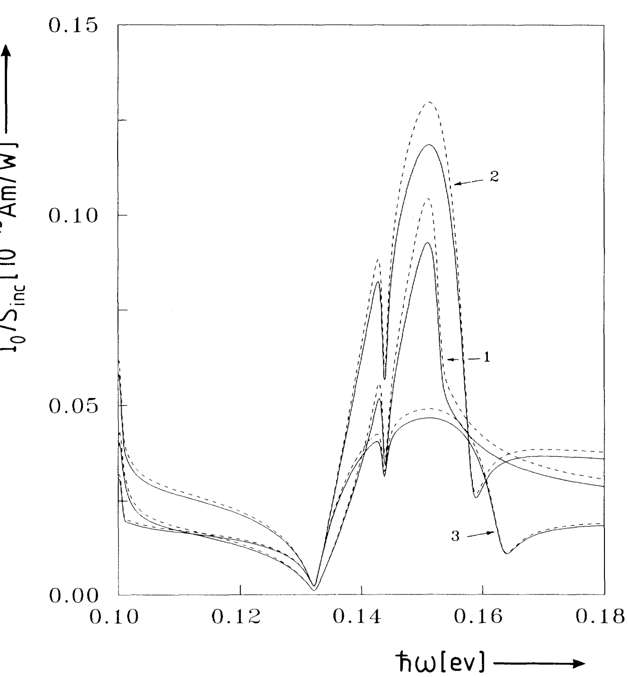

FIG. 3. Magnitude of the normalized integrated photon-drag current density (I_0/S_{inc}) as a function of the photon energy ($\hbar\omega$) for three different angles of incidence, viz., $\theta=20°$(1), 50°(2), and 70°(3). Fully drawn curves: slave model; dashed curves: self-field model. Excitation scheme: oblique incident bulk waves.

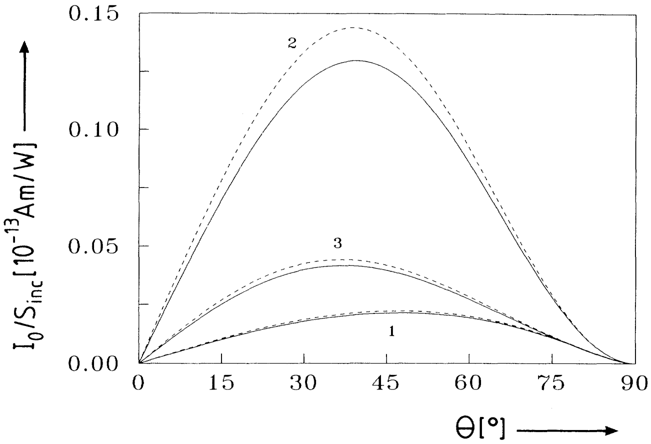

FIG. 4. Magnitude of the normalized integrated photon-drag current density (I_0/S_{inc}) as a function of the angle of incidence (θ) for three different photon energies, viz., $\hbar\omega=0.12$ eV (1), 0.15 eV (2), and 0.17 eV (3). Fully drawn curves: slave model; dashed curves: self-field model. Excitation scheme: oblique incident bulk waves.

B. Surface electromagnetic wave excitation of the drag current

One should anticipate the photon-drag effect to be resonantly enhanced if the excitation is caused by a p-

polarized surface electromagnetic wave (SEW). The formalism developed in the preceding sections can be applied also if the background field stems from a surface wave provided the backward coupling of the field from the surface to the source region is negligible, cf. Fig. 5. If the SEW is excited by means of the Otto prism configuration[22] the standard calculation for a three-layer (prism-vacuum-quartz) system shows that backcoupling is of no importance for an airgap (vacuum gap), D, a few times the decay length, α, of the incident field in the gap, i.e., $\alpha D \gtrsim 1$. In the gap, the Poynting vector of the incident field is parallel to the plane of the quantum well (see Fig. 5), $\mathbf{S}_{\rm inc}(z)=S_{\rm inc}(z)\mathbf{e}_x$, and just outside $(z=0^-)$ the quartz surface, and thus inside the quantum well the magnitude of the incident Poynting vector is given by

$$S_{\rm inc}(z=0^-)=\tfrac{1}{2}\epsilon_0\omega\frac{q_\parallel}{\alpha^2}|E^0_{1,x}(z=0^-)|^2 , \tag{76}$$

where

$$\alpha=\left[q_\parallel^2-\left[\frac{\omega}{c_0}\right]^2\right]^{1/2} , \tag{77}$$

and $E^0_{1,x}(z=0^-)$ is the x component of the incident field at the surface. Since $q_\parallel>\omega/c_0$ for the SEW, $\alpha=q^0_\perp/i$ is real and positive. The background field is related to $E^0_{1,x}(z=0^-)$ via

$$\frac{E^B_x(0)}{E^0_{1,x}(z=0^-)}=\frac{2\kappa_\perp}{q^0_\perp\epsilon_Q+\kappa_\perp} . \tag{78}$$

The ratio between the integrated photon-drag current density and the magnitude of the incident Poynting vector is obtained by combining Eqs. (66), (76), and (78). Thus,

$$\frac{I_0}{S_{\rm inc}(z=0^-)}=\frac{8\alpha^2|\kappa_\perp|^2}{\epsilon_0\omega q_\parallel|q^0_\perp\epsilon_Q+\kappa_\perp|^2}\frac{{\rm Re}K(q_\parallel,\omega)}{|1-K_{xx}(q_\parallel,\omega)|^2} . \tag{79}$$

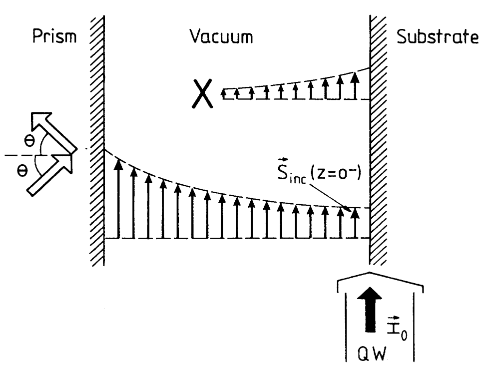

FIG. 5. Schematic illustration showing the electromagnetic Poynting vectors in the prism and vacuum regions, and the integrated photon-drag current density ($\mathbf{I}_0$). As indicated, the SEW-excited photon-drag current density is calculated under the assumption that there is no electromagnetic feedback on the source region.

The x component $q_\parallel$ of the wave vector is related to the angle of incidence θ at the prism-vacuum interface via $q_\parallel=n_P(\omega/c_0)\sin\theta$, n_P being the refractive index of the prism. For a given n_P, the quantity $c_0q_\parallel/\omega$ satisfies the inequalities $1\le c_0q_\parallel/\omega\le n_P$.

In Fig. 6 is shown the ratio $I_0/S_{\rm inc}(z=0^-)$ as a function of $c_0q_\parallel/\omega$ for five different frequencies ($\hbar\omega=0.134$, 0.136, 0.139, 0.141, and 0.144 eV). It appears from this figure that in the case of SEW excitation of the photon-drag effect the local-field effects are extremely important. Essentially, two local-field factors enter the denominator of Eq. (79). Thus, since the dispersion relation for a SEW on a bare vacuum-quartz interface is given by

$$q^0_\perp\epsilon_Q+\kappa_\perp=0 , \tag{80}$$

or, in explicit form, equivalently by the standard expression $q_\parallel=(\omega/c_0)[\epsilon_Q/(1+\epsilon_Q)]^{1/2}$, it is realized [see Eq. (79)] that the drag current density has a pronounced maximum when the background field is resonantly enhanced by SEW excitation. To stress the importance of the background resonance the dotted curves in Fig. 6 show $I_0/S_{\rm inc}(z=0^-)$ as a function of $c_0q_\parallel/\omega$ setting $K_{xx}=0$ (self-field approximation). In comparison to Fig. 7, in which the real and imaginary parts of the dispersion relation in Eq. (80) are shown, it appears that the broadening of the resonance with increasing light frequency stems

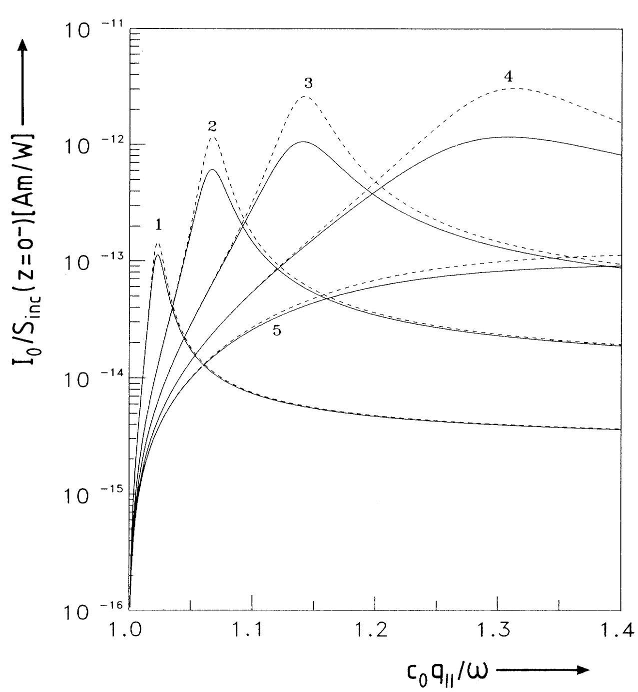

FIG. 6. Magnitude of the normalized integrated photon-drag current density $[I_0/S_{\rm inc}(z=0^-)]$ as a function of the normalized (real) wave vector $(c_0q_\parallel/\omega)$ parallel to the plane of the quantum well in the vicinity of the SEW resonance for five different photon energies, i.e., $\hbar\omega=0.134$ eV (1), 0.136 eV (2), 0.139 eV (3), 0.141 eV (4), and 0.144 eV (5). Fully drawn curves: slave model; dashed curves: self-field model.

from the fact that one moves into the damping region of the SEW as the frequency is increased. The local-field correction to the background field itself appears via the factor $|1-K_{xx}(q_{\parallel},\omega)|^2$ in the denominator of Eq. (79). Taking this correction into account also, the fully drawn curves of Fig. 6 show the result of the complete calculation of $I_0/S_{\rm inc}(z=0^-)$. Note that the self-consistent calculation reduces the integrated photon-drag current density by approximately a factor of 2 near resonance. The resonant behavior of $I_0/S_{\rm inc}(z=0^-)$ displayed by the fully drawn curves of Fig. 7 can be understood also as follows. Rewriting the product of the local-field factors in the form

$$|q_\perp^0\epsilon_Q+\kappa_\perp|^2|1-K_{xx}(q_\parallel,\omega)|^2 =|q_\perp^0\epsilon_Q+\kappa_\perp-N_{xx}(q_\parallel,\omega)q_\perp^0\kappa_\perp|^2 \,, \quad (81)$$

where

$$N_{xx}(q_\parallel,\omega)=-\frac{e^2}{\epsilon_0\omega}\left[\frac{\tau(\epsilon_F-\epsilon)}{\pi\hbar^2(1-i\omega\tau)}+\frac{2i\hbar^2(S_--S_+)}{m^2\omega}\right] , \quad (82)$$

Eq. (79) becomes

$$\frac{I_0}{S_{\rm inc}(z=0^-)}=\frac{8\alpha^2|\kappa_\perp|^2}{\epsilon_0\omega q_\parallel}\frac{{\rm Re}K(q_\parallel,\omega)}{|q_\perp^0\epsilon_Q+\kappa_\perp-N_{xx}q_\perp^0\kappa_\perp|^2} . \quad (83)$$

Now, since the condition

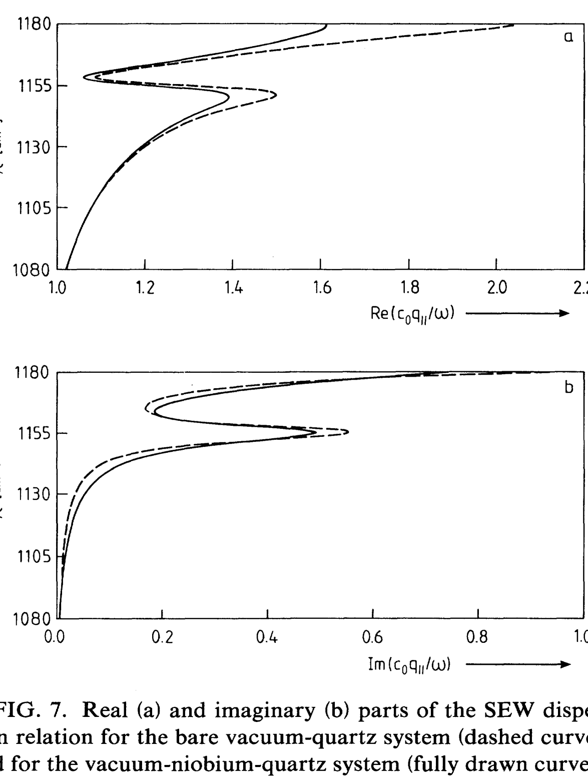

FIG. 7. Real (a) and imaginary (b) parts of the SEW dispersion relation for the bare vacuum-quartz system (dashed curves) and for the vacuum-niobium-quartz system (fully drawn curves). The reciprocal vacuum wavelength of light has been denoted by λ^{-1} and the SEW wave number ($q_\parallel$) is normalized by the vacuum wave number (ω/c_0).

$$q_\perp^0\epsilon_Q+\kappa_\perp=N_{xx}q_\perp^0\kappa_\perp \quad (84)$$

is precisely the dispersion relation for SEW's on the vacuum-Nb-quartz system,[4] it appears that the resonance behavior of $I_0/S_{\rm inc}(z=0^-)$ taking as a function of $c_0q_\parallel/\omega$ stems from the enhancement of the local field brought about by the Otto configuration excitations of the SEW in Eq. (84). The real and imaginary parts of the dispersion relation in Eq. (84) are plotted in Fig. 7. As one would expect for a 3-Å-thick quantum well, this dispersion relation deviates only slightly from that of the bare vacuum-quartz system far from the damping region. In the frequency range of interest here the last term in the square brackets of Eq. (82) gives a negligible contribution to the SEW dispersion relation. The increasing values of the half-widths of the curves in Fig. 6 with the electromagnetic frequency originate in the increasing of the damping as one moves into the dispersive part of the SEW dispersion relation. By comparison to the bulk excitation method considered in Sec. VI A it appears that SEW excitation causes an overall increase in the photon-drag current density by two orders of magnitude for the same incident field at the surface.

It is of interest to compare the SEW-enhanced photon-drag effect on a metallic quantum well (Nb-quartz) with the intersubband-resonant photon-drag effect of a semiconducting ($Al_xGa_{1-x}As/GaAs/Al_xGa_{1-x}As$) quantum well studied recently theoretically by Grinberg and Luryi[15] and experimentally by Wieck, Sigg, and Ploog.[16] In the limit of a large collisional broadening (small Doppler shift), which is appropriate from an experimental point of view, it is found[15,16] using an oblique illumination scheme that the normalized drag current is of the order of 10^{-5} mA cm/W near resonance, i.e., two orders of magnitude larger than the resonant values of Fig. 6. To obtain optical intersubband transitions for incident wavelengths in the vicinity of $\lambda_0\simeq 10$ μm, the quantum-well width must be of the order of 100 Å in the semiconducting system. In the present Nb-quartz structure the corresponding thickness is $d\sim 3$ Å. A further enhancement of the photon-drag effect can be obtained in the GaAs well if a multiple-quantum-well core is used in combination with a waveguide excitation scheme.

For the metallic quantum-well systems under study in this work it would be of importance to analyze the SEW-enhanced photon-drag effect as a function of the width of the quantum well. As the width increases more occupied levels occur in the well and as long as no interlevel transitions can occur (dominating diamagnetic coupling) one would expect a considerable increase in the normalized drag current with well thickness. At higher frequencies where the paramagnetic effects are important, pronounced resonances are expected to appear near the various two-level resonances even in a few monolayer thick quantum well. As in the semiconducting case multiple-quantum-well structures will lead to a further increase of the SEW-enhanced photon drag. It is obvious also that those (a few) monolayer thick metallic films (Ag and Au, for instance) having collision frequencies (far) less than that of Nb are of substantial interest for photon-drag studies among other things because a further enhancement of the SEW resonances is to be expected.

APPENDIX: LINEAR AND NONLINEAR CONDUCTIVITIES AT $T=0$ K

To obtain the result in Eq. (12) for the nonlinear conductivity tensor from Eq. (10), we assume that $\mathbf{q}_{\parallel}=q_{\parallel}\mathbf{e}_x$. With this choice the y component of the integral in Eq. (10) will vanish since the integrand is an uneven function of $k_{\parallel,y}=\mathbf{k}_{\parallel}\cdot\mathbf{e}_y$. This means that we only need to calculate the integral

$$I=\int_{-\infty}^{\infty}\frac{f_0\left[\epsilon+\frac{\hbar^2}{2m}|\mathbf{k}_{\parallel}-\mathbf{q}_{\parallel}|^2\right]-f_0\left[\epsilon+\frac{\hbar^2k_{\parallel}^2}{2m}\right]}{\hbar(\omega+i/\tau)+\frac{\hbar^2}{2m}|\mathbf{k}_{\parallel}-\mathbf{q}_{\parallel}|^2-\frac{\hbar^2k_{\parallel}^2}{2m}}\times(2k_{\parallel,x}-q_{\parallel})\frac{d^2k_{\parallel}}{(2\pi)^2}\ . \tag{A1}$$

Dividing this integral into two, viz., one containing $f_0[\epsilon+(\hbar^2/2m)|\mathbf{k}_{\parallel}-q_{\parallel}|^2]$ and one with $f_0[\epsilon+(\hbar^2k_{\parallel}^2/2m)]$, it is realized upon a change of variables $(\mathbf{k}\Longrightarrow\mathbf{k}_{\parallel}+\mathbf{q}_{\parallel})$ in the first integral that I can be written as

$$I=R_{-}-R_{+}\ , \tag{A2}$$

where

$$R_{\mp}=\int_{-\infty}^{\infty}\frac{f_0\left[\epsilon+\frac{\hbar^2k_{\parallel}^2}{2m}\right](2k_{\parallel,x}\pm q_{\parallel})}{\hbar(\omega+i/\tau)\mp\frac{\hbar^2q_{\parallel}^2}{2m}-\frac{\hbar^2}{m}k_{\parallel,x}q_{\parallel}}\frac{d^2k_{\parallel}}{(2\pi)^2}\ . \tag{A3}$$

In the low-temperature limit $f_0[\epsilon+(\hbar^2k_{\parallel}^2/2m)]=\theta[\epsilon_F-\epsilon-(\hbar^2k_{\parallel}^2/2m)]$, where θ is the Heaviside unit step function. Introducing polar coordinates, $(k_{\parallel,x},k_{\parallel,y})=k_{\parallel}(\cos\theta,\sin\theta)$, $R_{\mp}$ takes the following form at $T=0$ K:

$$R_{\mp}=\int_0^{\kappa_{\parallel}}\int_0^{2\pi}\frac{(2k_{\parallel}\cos\theta\pm q_{\parallel})k_{\parallel}d\theta\,dk_{\parallel}}{(2\pi)^2(\alpha_{\mp}-\beta k_{\parallel}\cos\theta)}\ , \tag{A4}$$

where $\alpha_{\mp}$, β, and $\kappa_{\parallel}$ are given by Eqs. (14)–(16). Carrying out, in turn, the integrations over θ and $\kappa_{\parallel}$, one obtains the results in Eq. (13).

As far as the linear conductivity tensor is concerned, it readily appears from Eq. (26) that the elements σ_{xy} and σ_{yx} will vanish (the relevent integrals are uneven functions of $k_{\parallel,y}$). Since also $\sigma_{xz}=\sigma_{zx}=\sigma_{yz}=\sigma_{zy}=0$, of course, $\overleftrightarrow{\sigma}$ has only diagonal elements. Among these diagonal elements, only σ_{xx} and σ_{yy} involve integrations over the $\mathbf{k}_{\parallel}$ plane. By comparing Eqs. (10) and (26), it is obvious that calculating σ_{yy} and σ_{xx} one needs to carry out the integrals

$$S_{\mp}=\int_{-\infty}^{\infty}\frac{f_0\left[\epsilon+\frac{\hbar^2k_{\parallel}^2}{2m}\right]k_{\parallel,y}^2}{\hbar(\omega+i/\tau)\mp\frac{\hbar^2q_{\parallel}^2}{2m}-\frac{\hbar^2}{m}k_{\parallel,x}q_{\parallel}}\frac{d^2k_{\parallel}}{(2\pi)^2} \tag{A5}$$

and

$$T_{\mp}=\int_{-\infty}^{\infty}\frac{f_0\left[\epsilon+\frac{\hbar^2k_{\parallel}^2}{2m}\right](2k_{\parallel,x}\pm q_{\parallel})^2}{\hbar(\omega+i/\tau)\mp\frac{\hbar^2q_{\parallel}^2}{2m}-\frac{\hbar^2}{m}k_{\parallel,x}q_{\parallel}}\frac{d^2k_{\parallel}}{(2\pi)^2}\ , \tag{A6}$$

respectively. By conversion to polar coordinates, one obtains in the low-temperature limit after a straightforward but tedious calculation precisely the results cited in Eqs. (32) and (33).

[1]E. V. Alieva, E. I. Firsov, L. A. Kuzik, V. A. Yakovlev, and F. A. Pudonin, Phys. Lett. A **152**, 89 (1991).

[2]M. Yamamoto and T. Namioka, Appl. Opt. **31**, 1612 (1992).

[3]O. Keller and A. Liu, Phys. Lett. A **167**, 301 (1993); **172**, 299 (1993).

[4]O. Keller and A. Liu (unpublished).

[5]G. L. Richmond, J. M. Robinson, and V. L. Shannon, Prog. Surf. Sci. **28**, 1 (1988).

[6]A. Liu and O. Keller, in *Proceedings of the Fifth International Topsøe Summer School on Nonlinear Optics,* edited by O. Keller (Nova Sciences, New York, 1993).

[7]J. M. Chen, J. R. Bower, C. S. Wang, and C. H. Lee, Opt. Commun. **9**, 132 (1973).

[8]J. F. McGilp, J. Vac. Sci. Technol. A **5**, 1442 (1987).

[9]K. J. Song, D. Heskett, H. L. Dai, A. Liebsch, and E. Plummer, Phys. Rev. Lett. **61**, 1380 (1988).

[10]M. P. C. M. Krijn and B. J. Geurts, Phys. Rev. B **44**, 10 712 (1991).

[11]S. Lindgren and L. Walldén, Phys. Rev. B **45**, 6345 (1992).

[12]O. Keller, in *Proceedings of the Fifth International Topsøe Summer School on Nonlinear Optics* (Ref. 6).

[13]F. T. Vas'ko, Fiz. Tekh. Poluprovodn. **19**, 1319 (1985) [Sov. Phys. Semicond. **19**, 808 (1985)].

[14]S. Luryi, Phys. Rev. Lett. **58**, 2263 (1987).

[15]A. A. Grinberg and S. Luryi, Phys. Rev. B **38**, 87 (1988).

[16]A. D. Wieck, H. Sigg, and K. Ploog, Phys. Rev. Lett. **64**, 463 (1990).

[17]M. I. Stockman, L. N. Pandey and T. F. George, Phys. Rev. Lett. **65**, 3433 (1990).

[18]V. M. Shalaev, C. Douketis, and M. Moskovits, Phys. Lett. A **169**, 205 (1992).

[19]R. Kesselring, A. W. Kälin, H. Sigg, and F. K. Kneubühl, Rev. Sci. Instrum. **63**, 3317 (1992).

[20]O. Keller, Phys. Rev. B **42**, 6049 (1990).

[21]F. Gervais and B. Piriou, Phys. Rev. B **11**, 3944 (1975).

[22]A. Otto, Z. Phys. **216**, 398 (1968).